Pathology

Pathology International 2012; **62**: 219–225 doi:10.1111/j.1440-1827.2011.02779.x

Original Article

CD44 expression in plexiform lesions of idiopathic pulmonary arterial hypertension

Keiko Ohta-Ogo,[1,2] Hiroyuki Hao,[2,3] Hatsue Ishibashi-Ueda,[2] Seiichi Hirota,[3] Kazufumi Nakamura,[1] Tohru Ohe[1] and Hiroshi Ito[1]

[1]*Department of Cardiovascular Medicine, Okayama University Graduate School of Medicine, Dentistry and Pharmaceutical Sciences, Kita-ku, Okayama,* [2]*Department of Pathology, National Cerebral and Cardiovascular Center, Suita, Osaka and* [3]*Department of Surgical Pathology, Hyogo College of Medicine, Nishinomiya, Hyogo, Japan*

Plexiform lesions in pulmonary arteries are a characteristic histological feature for idiopathic pulmonary arterial hypertension (IPAH). The pathogenesis of the plexiform lesion is not fully understood, although it may be related to endothelial cell dysfunction and local inflammation. CD44 is a cell adhesion molecule and it is also involved in angiogenesis, endothelial cell proliferation and migration. The expression of CD44 was examined in lung plexiform lesions obtained from patients with IPAH (IPAH group, $n = 7$) and pulmonary arterial hypertension associated with atrial septal defect (ASD-PAH group, $n = 4$). Expression of CD44 was detected in 49 out of 52 plexiform lesions (93%) from all patients in the IPAH group, whereas 31 plexiform lesions obtained from the ASD-PAH group lacked CD44 positivity by immunohistochemistry. In the IPAH group, CD44 was localized in the endothelial cells of microvessels within plexiform lesions and activated T cells in and around the lesions. Furthermore, T cell infiltration and endothelial cell proliferation activity were prominent in the plexiform lesions of the IPAH group, compared to those of the ASD-PAH group. These findings suggest that CD44 and activated T cell infiltration play an important role in the development of plexiform lesions particularly in IPAH.

Key words: CD44, endothelial cell, plexiform lesion, pulmonary arterial hypertension

Idiopathic pulmonary arterial hypertension (IPAH) is a rare disorder, characterized by sustained elevation of pulmonary arterial pressure without a demonstrable cause.[1] Although the discovery of the mutations in the gene encoding the bone morphogenetic protein receptor type II (BMPR2) in patients with familial pulmonary arterial hypertension (PAH)[2,3] and sporadic IPAH[4] emphasized the importance of BMP/TGF-β signaling, the pathogenesis of IPAH has not been fully clarified. The underlying mechanism is pulmonary vascular remodeling involving the pre- and intra-acinar pulmonary arteries: (i) constrictive lesions such as intimal thickening and medial hypertrophy and (ii) complex lesions characterized by plexiform lesions.[5] The plexiform lesion has been highlighted in pulmonary arteriopathy of IPAH, because it is not only a marker of severity or rapid progression of pulmonary hypertension,[6] but also has contributed to pathogenesis of the disease, particularly with regard to endothelial cell abnormalities and inflammation.

Morphologically, the plexiform lesion is a focal proliferation of endothelial channels lined by myofibroblasts, smooth muscle cells, and connective tissue matrix in an aneurysmal dilatation of muscular pulmonary artery branches associated with partial destruction of the vessel wall.[5,7] Previously, evidence of endothelial dysfunction,[8,9] one of the key pathogeneses of IPAH, as well as endothelial cell proliferation[7,10,11] and disordered angiogenesis[12] have been shown in plexiform lesions. In addition to endothelial abnormalities, frequent inflammatory infiltrates such as lymphocytes and macrophages have been identified in plexiform lesions,[7] suggesting that inflammatory mechanisms also play an important role in the pathogenesis of IPAH. This view has been supported by the frequent presence of autoantibodies such as circulating antinuclear antibodies and elevated circulating levels of proinflammatory cytokines[13] and chemokines[14] in IPAH patients. Moreover, increased fractalkine expression in PAH lungs and its receptor on circulating T cells[15] as well as increased expression of chemokine RANTES (regulated

Correspondence: Hiroyuki Hao, MD, PhD, Department of Surgical Pathology, Hyogo College of Medicine, 1-1, Mukogawa-cho, Nishinomiya, Hyogo 663-8501, Japan. Email: haohiro@hyo-med.ac.jp

Received 26 September 2011. Accepted for publication 25 November 2011.

upon activation, normal T-cell expressed and secreted) predominantly in plexiform lesions associated with CD45-positive cell infiltrates[16] emphasize a role of inflammatory cell recruitment in this disorder.

CD44 is a member of the hyaluronate (HA) receptor family of cell adhesion molecules involved in leukocyte trafficking.[17,18] This molecule can mediate the adhesion of lymphocytes to vascular endothelial cells via binding of HA and the extravasation of activated T cells into sites of inflammation in mice[19] and in human autoimmune disease.[20] In addition, CD44 is involved in endothelial cell proliferation, migration and angiogenesis[21,22] that are the characteristic features of plexiform lesions in IPAH.

In light of these functions, we hypothesized that CD44 might be involved in the progressive vascular remodeling, particularly in plexiform lesions of patients with IPAH. The purpose of the present study was to begin an exploration of the potential roles of CD44 in the pathogenesis of IPAH by determining the immunohistochemical expression and localization of CD44 in the plexiform lesions and associated T cell recruitment.

MATERIALS AND METHODS

Case materials

Formalin-fixed, paraffin-embedded blocks of lung tissue displaying plexogenic pulmonary arteriopathy were retrieved from the archival collection of the Department of Pathology, National Cerebral and Cardiovascular Center, Suita, Japan, apart from two cases provided by the Department of Cardiovascular Medicine, Okayama University Graduate School of Medicine, Dentistry, and Pharmaceutical Science, Okayama, Japan. Seven cases of IPAH (6 women, 1 man, mean age 31 ± 5 years old, mean pulmonary arterial pressure (PAP) 64 ± 4 mmHg) were entered into the study.

To compare CD44 expression between idiopathic and non-idiopathic cases, four cases of PAH associated with atrial septal defect (ASD-PAH) (3 women, 1 man, mean age 28 ± 9 years old, mean PAP 63 ± 4 mmHg) were also included. Clinical classification of PAH patients was according to Dana Point Classification[23] and the patients' clinical information is presented in Table 1. The patients were all nonsmokers, and were without known risk factors or associated conditions of PAH[23] such as appetite suppressants, connective tissue diseases, human immunodeficiency virus infection, portal hypertension, congenital heart disease (except ASD-PAH cases), schistosomiasis, chronic hemolytic anemia or chronic parenchymal lung disease. All cases originated from autopsy material, except two lung specimens from Okayama University (one with IPAH and the other with ASD-PAH) obtained at the time of lung transplantation. Two blocks for each lobe of bilateral lungs were prepared randomly in each case. Plexiform lesions were identified and counted on hematoxylin and eosin stained sections. Normal lung tissues from three autopsy cases (1 woman, 2 men, mean age 52 ± 20 years old) with no cardiac or pulmonary disease were used as controls.

Immunohistochemistry

Each paraffin-embedded block including plexiform lesions was serially cut into three-micrometer thick sections. The sections were pre-incubated with blocking reagent to quench endogenous peroxidase activity, followed by incubation with the primary antibodies at room temperature, except when otherwise noted. The antibody for CD44 (1:25, Dako, Glostrup, Denmark) was incubated at 4°C overnight. The antibodies for CD31 (1:50, Dako) for endothelial cells, CD68 (1:50,

Table 1 Clinical classification and information of the PAH patients

Patients	Sex	Age	mPAP (mmHg)	CI (L/min/m^2)	Risk factors* for PAH	ANA	iv PGI_2	Cause of death	Lung specimen
IPAH1	F	18	58	1.7	None	Negative	–	Right heart failure	Autopsy
IPAH2	F	32	62	1.6	None	Negative	+	Right heart failure	Autopsy
IPAH3	F	43	72	2.6	None	Negative	+	Alive (LTx)	LTx
IPAH4	F	26	78	1.6	None	Negative	–	Right heart failure	Autopsy
IPAH5	M	54	71	1.9	None	Negative	–	Right heart failure	Autopsy
IPAH6	F	12	45	3.0	None	Negative	–	Right heart failure	Autopsy
IPAH7	F	34	63	0.8	None	Negative	+	Right heart failure	Autopsy
ASD-PAH1	F	51	54	NA	CHD	NA	–	Sudden arrest	Autopsy
ASD-PAH2	M	13	71	NA	CHD	NA	–	Right heart failure	Autopsy
ASD-PAH3	F	32	61	2.3	CHD	NA	–	Infective endocarditis	Autopsy
ASD-PAH4	F	16	65	2.5	CHD	Negative	+	Alive (LTx)	LTx

*Known risk factors and associated conditions of PAH such as appetite suppressants, connective tissue diseases, human immunodeficiency virus infection, portal hypertension, congenital heart diseases, schistosomiasis, and chronic hemolytic anemia.[23]

ANA, indicates anti-nuclear antibody; ASD-PAH, pulmonary arterial hypertension associated with atrial septal defect; CHD, congenital heart diseases; CI, cardiac index; IPAH idiopathic pulmonary arterial hypertension; iv PGI_2, intravenous prostacyclin treatment; LTx, lung transplantation; mPAP, mean pulmonary arterial pressure; NA, not available.

Dako) for macrophages, CD45RO (1:100, Dako) for T lymphocytes, α-smooth muscle actin (α-SMA, 1:100, Dako) for smooth muscle cells, and Ki-67 (1:150, Dako) for evaluation of proliferation activity were incubated for 60 min. The EnVision+ System (Dako) was employed for visualization. Immunohistochemistry for CD44 was evaluated as the ratio of the number of plexiform lesions including CD44-positive cells per total number of lesions in each case. To identify cell types corresponding to CD44-positive elements, we proceeded with a sequence of immunohistochemical reactions using the combination of CD44 antibody and one of the following antibodies; CD31, CD68, CD45RO, or α-SMA, in the same section.

Statistical analysis

Fisher's protected least significant difference (PLSD) test and Mann–Whitney *U*-test were used to compare the IPAH, ASD-PAH, and control groups. Mean values (±SEM) are presented in the text.

RESULTS

Detection of plexiform lesions in lung tissue

The histology of lung tissue from the IPAH and ASD-PAH patients showed similar pulmonary artery remodeling, consisting of medial hypertrophy, intimal fibrosis, and plexiform lesions. We found 83 plexiform lesions, which were composed of 52 lesions from the IPAH group and 31 lesions from the ASD-PAH group (Table 2). From three to 12 plexiform lesions in the lung sections were detected per patient. On the other hand, control lung sections were confirmed to show no evidence of either pulmonary artery remodeling or interstitial inflammation.

Table 2 Distribution of CD44-positive plexiform lesions in the lung specimens of IPAH and ASD-PAH patients

Patients	Number of plexiform lesions studied (A)	Number of CD44 positive lesions (B)	B/A (%)
IPAH1	6	5	83.3
IPAH2	6	6	100
IPAH3	6	6	100
IPAH4	7	5	71.4
IPAH5	8	8	100
IPAH6	12	12	100
IPAH7	7	7	100
ASD-PAH1	12	0	0
ASD-PAH2	5	0	0
ASD-PAH3	11	0	0
ASD-PAH4	3	0	0

ASD-PAH, indicates pulmonary arterial hypertension associated with atrial septal defect; IPAH, idiopathic pulmonary arterial hypertension.

Immunohistochemical expression and localization of CD44 protein in plexiform lesions

Immunohistochemistry was performed with lung tissue from IPAH and ASD-PAH patients to determine the presence of CD44 in plexiform lesions. Staining for CD44 was detected in 49 out of 52 plexiform lesions (93%) from all patients with IPAH, ranging from 71.4 to 100% of lesions per patient, whereas plexiform lesions from ASD-PAH group did not show CD44 positivity (Table 2). In the IPAH group, the CD44-positive cells were apparently localized along the surface of thin-walled microvessels within plexiform lesions and infiltrating mononuclear cells in and around the lesions (Fig. 1a,b). Alpha-SMA-positive smooth muscle cells did not show CD44 positivity in the plexiform lesions (Data not shown). Some endothelial cells of constrictive lesions giving rise to plexiform lesions also showed CD44 positivity. Otherwise, CD44 was not expressed in vascular lesions apart from plexiform lesions, in spite of their constrictive vascular lesions (Fig. 1c,d). Immunohistochemistry was also performed with control lungs to examine whether CD44 was expressed in normal pulmonary arteries without remodeling. CD44 immunostaining was not observed in any vascular cell components of normal pulmonary arteries although a small number of alveolar macrophages were stained. Double-labeling immunohistochemistry revealed CD44-positive cells mainly corresponded to CD31-positive cells and CD45RO-positive cells, indicating that they were endothelial cells and activated T-cells, respectively (Fig. 2a,b). Serial sections of the plexiform lesions from IPAH and ASD-PAH revealed that a vast majority of CD44-positive cells (Fig. 3a) in IPAH plexiform lesion were CD45RO-positive T cells (Fig. 3b), not CD68-positive macrophages (Fig. 3c). Macrophages were also infiltrated in ASD-PAH (Fig. 3f) plexiform lesions. However, lack of immune-reaction against CD44 was apparent (Fig. 3d) and few T cells were identified (Fig. 3e) in the ASD-PAH plexiform lesion.

Inflammatory cell infiltration surrounding plexiform lesions in IPAH

In order to evaluate CD44 expression in IPAH but not in ASD-PAH, the numbers of CD45RO-positive T cell and CD68-positive macrophage inflammation per plexiform lesion for IPAH and ASD-PAH group and per normal small pulmonary artery for control group were counted. Consecutive sections showed that CD45RO-positive cells surrounding plexiform lesions were significantly increased in IPAH group compared to those in ASD-PAH (20.6 ± 1.8 versus 4.3 ± 1.3 per lesion, $P < 0.05$, Fig. 4). Plexiform lesions in ASD-PAH group included a small number of CD45RO-positive cells as

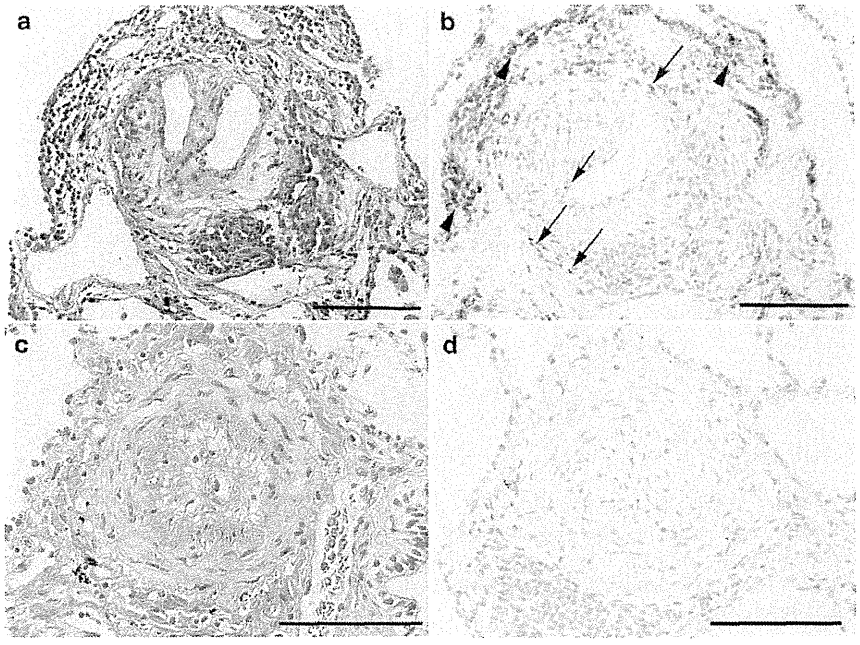

Figure 1 Hematoxylin and eosin and immunohistochemistry of CD44 in (a, b) a plexiform lesion and (c, d) a constrictive vascular lesion of a patient with idiopathic pulmonary arterial hypertension were shown. CD44 was clearly positive on the surface of thin-walled microvessels within the plexiform lesion (b; arrows) and perivascular infiltrating round cells (b; arrowheads). CD44 was not expressed in a constrictive lesion apart from plexiform lesions (d). (a-d; Scale bar 50 μm)

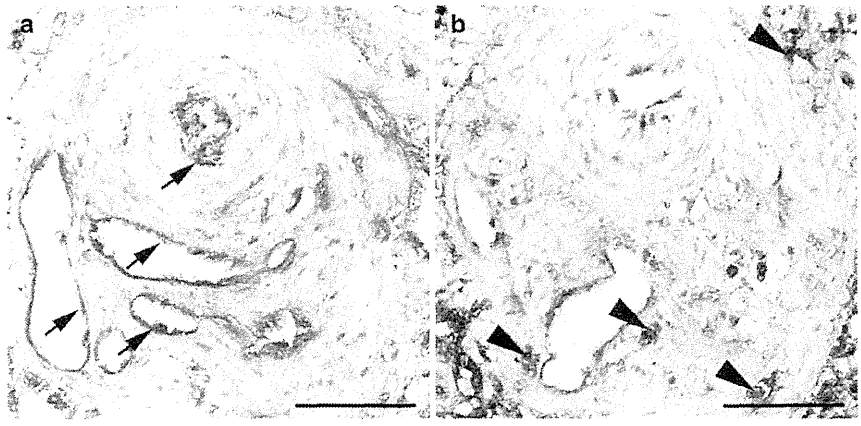

Figure 2 Double-labeling immunohistochemistry demonstrated presence of both CD44 (brown) and CD31 (red) positive cells (a; arrows) in a plexiform lesion obtained from a patient with idiopathic pulmonary arterial hypertension. Double-labeling cells of CD44 (brown) and CD45RO (red) were also evident in the same lesion (b; arrowheads). (a, b; Scale bar 50 μm)

little as control group (4.9 ± 2.4 per artery, NS). In contrast, the number of CD68-positive macrophage was similar in the IPAH group compared to those in the ASD-PAH group (10.9 ± 2.0 versus 17.5 ± 2.6 per lesion, $P = 0.50$). A few CD68-positive macrophages were observed in small pulmonary arteries obtained from normal lung tissue (0.8 ± 2.0 per artery).

Proliferation activity of endothelial cell in plexiform lesions

In order to evaluate the proliferative activity for endothelial cell of plexiform lesions in IPAH group and ASD-PAH group, immunohistochemistry for Ki-67 was examined. The number of Ki-67-positive cells in the plexiform lesions of IPAH patients was significantly higher, compared to those of the ASD-PAH group (4.2 ± 1.0 versus 0.8 ± 0.5 per lesion, $P < 0.05$, Fig. 5).

DISCUSSION

The present study demonstrated for the first time that CD44 protein was frequently expressed in plexiform lesions in the lungs from patients with IPAH and mainly localized in the endothelial cells composing microvessels of the lesions and surrounding T cells. In addition, the plexiform lesions of the IPAH group were accompanied by significant T cell infiltration. In contrast, the plexiform lesions in patients with ASD-PAH did not show detectable CD44 nor significant T cell infiltrates. These findings suggest that CD44 plays some role in the development of plexiform lesions, particularly in IPAH, presumably associated with persistent T cell inflammation.

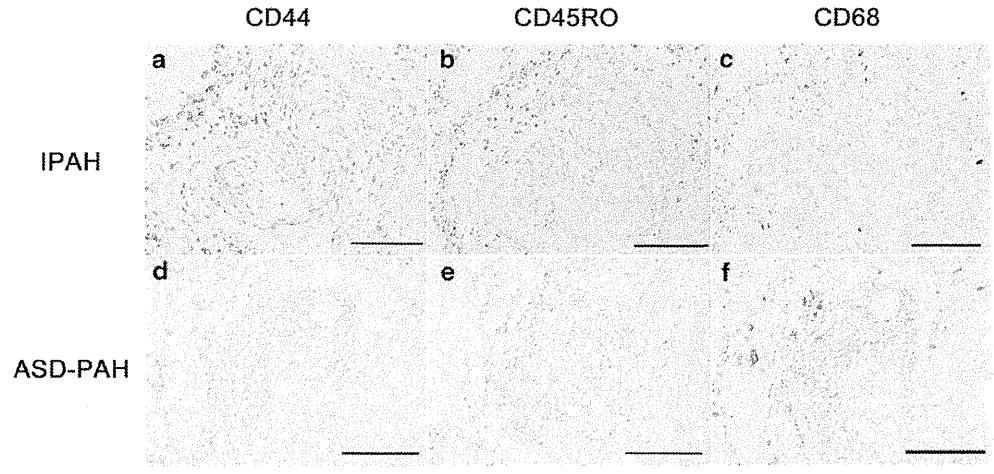

Figure 3 Immunohistochemistry of CD44, CD45RO and CD68 in the serial sections of plexiform lesion from patients with idiopathic pulmonary arterial hypertension (IPAH) and pulmonary artery hypertension associated with atrial septal defect (ASD-PAH) were shown. A vast majority of (a) CD44-positive cells in IPAH plexiform lesion were (b) T cells, not (c) CD68-positive macrophages. Macrophages were also infiltrated in (f) ASD-PAH plexiform lesions, whereas (d) lack of immune-reaction against CD44 was apparent and few T cells were identified (e) in the ASD-PAH plexiform lesion. (a-f; Scale bar 50 μm)

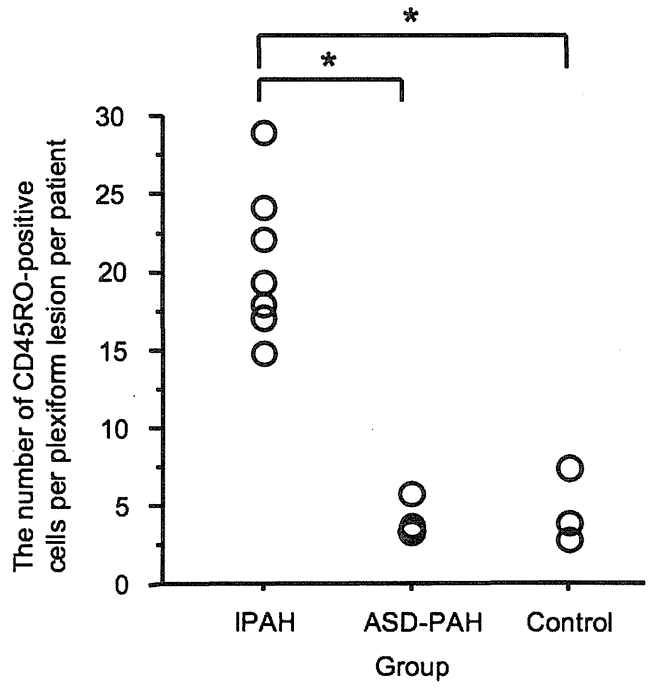

Figure 4 The chart showed the mean number of CD45RO-positive T cells per plexiform lesion in patients with idiopathic pulmonary artery hypertension (IPAH), pulmonary artery hypertension associated with atrial septal defect (ASD-PAH), and per normal small pulmonary artery in control group. Number of CD45RO-positive T cells was significantly higher in and around plexiform lesions of patients with IPAH, compared to that of ASD-PAH and normal small pulmonary arteries. (*$P < 0.01$)

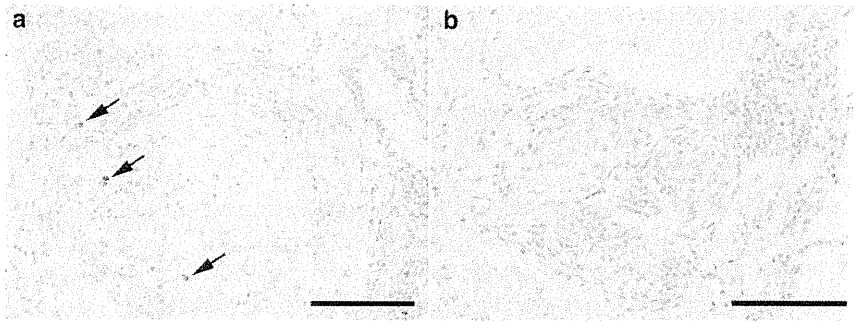

Figure 5 Immunohistochemistry of Ki-67 in plexiform lesions of a patient with idiopathic pulmonary arterial hypertension (IPAH) and pulmonary arterial hypertension associated with atrial septal defect (ASD-PAH) was shown. A certain subset of endothelial cells of IPAH plexifom lesion was apparently positive for Ki-67 immunohistochemistry (a; arrows), whereas most of the endothelial cells in the ASD-PAH plexiform lesions lacked immunoreactivity against Ki-67 (b). (a, b; Scale bar 50 μm)

CD44 is involved in cell-cell and cell-matrix interaction, and presumably maintains organ and tissue structures under normal conditions.[18] On the other hand, CD44 is shown to contribute to many pathological conditions including inflammation and autoimmune diseases, angiogenesis, atherosclerosis,[24] and malignancies and tumor metastases, via its multiple functions.

Our data implies CD44 involvement in the mechanism of persistent local inflammation observed in plexiform lesions in IPAH. Inflammatory mechanisms including inflammatory cell recruitment have become increasingly important in IPAH.[7,13–16] In the current study, CD44 expression was shown to localize in endothoelial cells and T cells in IPAH plexiform lesions. This was accompanied by significant T cell infiltration that was consistent with previous observation by other researchers.[7,16] CD44 is a homing receptor for leukocytes and required for activated T cell extravasation into an inflammatory site.[19] Increased surface levels of CD44 proteins are characteristic of T cell activation after encounter with its cognate antigen.[25] On the other hand, chronic inflammation increases CD44 expression on T cells[26] and endothelial cells express CD44 after exposure to proinflammatory cytokines such as IL-1β and TNF-α.[24] Thus, CD44 may be involved in ongoing local inflammatory processes in IPAH through T cell and endothelial cell activation and inflammatory cell recruitment.

Our data also suggests that a subset of the endothelial cells in plexiform lesions in IPAH are activated and involved in angiogenesis. CD44 is an activation marker of endothelial cells because normal endothelial cells were shown to express no or low levels of CD44, but expression is up-regulated in growing cells by activation, for example, with cytokines,[24] and by isolating and culturing of these cells or in tumor associated endothelial cells responsible for tumor angiogenesis.[22] One possible explanation for this activation is stimulation by angiogenic factors, because basic fibroblast growth factor and vascular endothelial growth factor (VEGF) are shown to upregulate CD44 expression on cultured human endothelial cells,[22] on the other hand, there is evidence of increased expression of angiogenesis-related molecules including VEGF and its receptors in endothelial cells within plexiform lesions in severe PAH.[10,12] However, other mechanisms may exist. In addition, the presence of proliferating endothelial cells by Ki-67 labeling in plexiform lesions in IPAH is in keeping with previous observation showing Ki-67-positive endothelial cells in plexiform lesions accompanied by inflammatory cells in pulmonary hypertension associated with scleroderma and human immunodeficiency virus infection.[27] Our findings support the view that endothelial cells of IPAH plexiform lesion may be prone to proliferation and these results suggest the activated stage of disease in IPAH patients.

The principle ligand of CD44 is HA.[17] Recently, two groups independently reported data suggesting an involvement of HA in the pathogenesis of IPAH. Aytekin *et al.* showed patients with IPAH had higher circulating levels of HA[28] and Papakonstantinou *et al.* showed a significant increase in HA content in IPAH lungs compared with donor.[29] Both groups showed intense HA staining in and around remodeled vessels and indicated increased HA production in pulmonary artery smooth muscle cells (PASMC) derived from IPAH lungs. In addition, PASMCs from IPAH had increased binding of mononuclear cells compared with controls.[28] These data suggests a role for HA in remodeling and inflammation via enhanced HA production in PASMC in IPAH. Because CD44 is the principle receptor for HA and its interaction regulates important processes such as cell migration, proliferation, leukocyte trafficking and activation, it is plausible that HA effects on remodeling and inflammation are mediated, at least in part, by CD44. Interestingly, data by the latter group also included significantly increased CD44 mRNA expression measured by quantitative RT-PCR in IPAH lungs compared with donor lungs,[29] in keeping with our data of increased immunohistochemical expression of CD44 in IPAH.

The intriguing finding in this study was that the plexiform lesions from the patients with ASD-PAH lacked immunohistochemical CD44 expression and were less inflamed with regard to T cells despite the similarity of morphological and hemodynamic features to IPAH. Although a relatively large number of plexiform lesions was examined, because of the limited number of patients with ASD-PAH available, the further investigation is needed to confirm the lack of CD44 in this group. However, the finding implies the difference in CD44 expression may result from different underlying pathogeneses. In fact, researchers have pointed out some distinctions between plexiform lesions in IPAH and those in congenital left-to-right shunts including ASD-PAH.[5] Importantly, in IPAH, the endothelial cell proliferation in plexiform lesions was found to be mainly monoclonal, whereas in secondary PH associated with congenital heart disease with left-to-right shunts and CREST syndrome, it was polyclonal, suggesting underlying pathogenetic mechanisms are distinct.[11] That is, monoclonal endothelial cell proliferation in IPAH is autonomous growth, more closely related to cancer cells, on the other hand, polyclonal proliferation in secondary PH is as a response to exogenous stimuli like high shear stress.[11] CD44 may be associated with abnormalities causing monoclonal expansion in IPAH, though the mechanism is yet to be determined. It will be of interest to expand our investigation to plexiform lesions in other PAH associated with underlying diseases.

Lastly, whether the IPAH patients in this study carried the BMPR2 mutation was not determined since the genetic test was not available. However the presence of inflammation would not be necessarily inconsistent with the mutation with regard to the development of the disease, because inflammatory mechanisms are now thought to be an important factor in subjects with the mutations. Heterozygous BMPR2 mutant mice develop pulmonary hypertension not spontaneously but

under inflammatory stress.[30] In addition, a complete negative feedback loop between IL-6 and BMP both *in vitro* and *in vivo* have been shown, suggesting that an important consequence of BMPR2 mutations may be poor regulation of cytokines and thus vulnerability to an inflammatory second hit.[31]

In conclusion, this study provides novel observation on the expression of CD44 predominantly in endothelial cells composing plexiform lesions and surrounding T cells in patients with IPAH, not in ASD-PAH, accompanied by significant T cell infiltration. These data suggest involvement of CD44 in the pathogenesis of IPAH, presumably associated with endothelial cell activation and persistent local inflammation.

REFERENCES

1 Rubin LJ. Primary pulmonary hypertension. *N Engl J Med* 1997; **336**: 111–7.
2 Machado RD, Pauciulo MW, Thomson JR *et al.* BMPR2 haploinsufficiency as the inherited molecular mechanism for primary pulmonary hypertension. *Am J Hum Genet* 2001; **68**: 92–102.
3 Newman JH, Wheeler L, Lane KB *et al.* Mutation in the gene for bone morphogenetic protein receptor II as a cause of primary pulmonary hypertension in a large kindred. *N Engl J Med* 2001; **345**: 319–24.
4 Thomson JR, Machado RD, Pauciulo MW *et al.* Sporadic primary pulmonary hypertension is associated with germline mutations of the gene encoding BMPR-II, a receptor member of the TGF-beta family. *J Med Genet* 2000; **37**: 741–5.
5 Pietra GG, Capron F, Stewart S *et al.* Pathologic assessment of vasculopathies in pulmonary hypertension. *J Am Coll Cardiol* 2004; **43**: 25S–32S.
6 Pietra GG, Edwards WD, Kay JM *et al.* Histopathology of primary pulmonary hypertension. A qualitative and quantitative study of pulmonary blood vessels from 58 patients in the National Heart, Lung, and Blood Institute, Primary Pulmonary Hypertension Registry. *Circulation* 1989; **80**: 1198–206.
7 Tuder RM, Groves B, Badesch DB, Voelkel NF. Exuberant endothelial cell growth and elements of inflammation are present in plexiform lesions of pulmonary hypertension. *Am J Pathol* 1994; **144**: 275–85.
8 Tuder RM, Cool CD, Geraci MW *et al.* Prostacyclin synthase expression is decreased in lungs from patients with severe pulmonary hypertension. *Am J Respir Crit Care Med* 1999; **159**: 1925–32.
9 Giaid A, Yanagisawa M, Langleben D *et al.* Expression of endothelin-1 in the lungs of patients with pulmonary hypertension. *N Engl J Med* 1993; **328**: 1732–9.
10 Cool CD, Stewart JS, Werahera P *et al.* Three-dimensional reconstruction of pulmonary arteries in plexiform pulmonary hypertension using cell-specific markers. Evidence for a dynamic and heterogeneous process of pulmonary endothelial cell growth. *Am J Pathol* 1999; **155**: 411–9.
11 Lee SD, Shroyer KR, Markham NE, Cool CD, Voelkel NF, Tuder RM. Monoclonal endothelial cell proliferation is present in primary but not secondary pulmonary hypertension. *J Clin Invest* 1998; **101**: 927–34.
12 Tuder RM, Chacon M, Alger L *et al.* Expression of angiogenesis-related molecules in plexiform lesions in severe pulmonary hypertension: Evidence for a process of disordered angiogenesis. *J Pathol* 2001; **195**: 367–74.
13 Humbert M, Monti G, Brenot F *et al.* Increased interleukin-1 and interleukin-6 serum concentrations in severe primary pulmonary hypertension. *Am J Respir Crit Care Med* 1995; **151**: 1628–31.
14 Itoh T, Nagaya N, Ishibashi-Ueda H *et al.* Increased plasma monocyte chemoattractant protein-1 level in idiopathic pulmonary arterial hypertension. *Respirology* 2006; **11**: 158–63.
15 Balabanian K, Foussat A, Dorfmuller P *et al.* CX(3)C chemokine fractalkine in pulmonary arterial hypertension. *Am J Respir Crit Care Med* 2002; **165**: 1419–25.
16 Dorfmuller P, Zarka V, Durand-Gasselin I *et al.* Chemokine RANTES in severe pulmonary arterial hypertension. *Am J Respir Crit Care Med* 2002; **165**: 534–9.
17 Aruffo A, Stamenkovic I, Melnick M, Underhill CB, Seed B. CD44 is the principal cell surface receptor for hyaluronate. *Cell* 1990; **61**: 1303–13.
18 Goodison S, Urquidi V, Tarin D. CD44 cell adhesion molecules. *Mol Pathol* 1999; **52**: 189–96.
19 DeGrendele HC, Estess P, Siegelman MH. Requirement for CD44 in activated T cell extravasation into an inflammatory site. *Science* 1997; **278**: 672–5.
20 Estess P, DeGrendele HC, Pascual V, Siegelman MH. Functional activation of lymphocyte CD44 in peripheral blood is a marker of autoimmune disease activity. *J Clin Invest* 1998; **102**: 1173–82.
21 Trochon V, Mabilat C, Bertrand P *et al.* Evidence of involvement of CD44 in endothelial cell proliferation, migration and angiogenesis in vitro. *Int J Cancer* 1996; **66**: 664–8.
22 Griffioen AW, Coenen MJ, Damen CA *et al.* CD44 is involved in tumor angiogenesis; an activation antigen on human endothelial cells. *Blood* 1997; **90**: 1150–59.
23 Simonneau G, Robbins IM, Beghetti M *et al.* Updated clinical classification of pulmonary hypertension. *J Am Coll Cardiol* 2009; **54**: S43–54.
24 Krettek A, Sukhova GK, Schonbeck U, Libby P. Enhanced expression of CD44 variants in human atheroma and abdominal aortic aneurysm: Possible role for a feedback loop in endothelial cells. *Am J Pathol* 2004; **165**: 1571–81.
25 DeGrendele HC, Kosfiszer M, Estess P, Siegelman MH. CD44 activation and associated primary adhesion is inducible via T cell receptor stimulation. *J Immunol* 1997; **159**: 2549–53.
26 Siegelman MH, DeGrendele HC, Estess P. Activation and interaction of CD44 and hyaluronan in immunological systems. *J Leukoc Biol* 1999; **66**: 315–21.
27 Cool CD, Kennedy D, Voelkel NF, Tuder RM. Pathogenesis and evolution of plexiform lesions in pulmonary hypertension associated with scleroderma and human immunodeficiency virus infection. *Hum Pathol* 1997; **28**: 434–42.
28 Aytekin M, Comhair SA, de la Motte C *et al.* High levels of hyaluronan in idiopathic pulmonary arterial hypertension. *Am J Physiol Lung Cell Mol Physiol* 2008; **295**: L789–99.
29 Papakonstantinou E, Kouri FM, Karakiulakis G, Klagas I, Eickelberg O. Increased hyaluronic acid content in idiopathic pulmonary arterial hypertension. *Eur Respir J* 2008; **32**: 1504–12.
30 Song Y, Jones JE, Beppu H, Keaney JF Jr, Loscalzo J, Zhang YY. Increased susceptibility to pulmonary hypertension in heterozygous BMPR2-mutant mice. *Circulation* 2005; **112**: 553–62.
31 Hagen M, Fagan K, Steudel W *et al.* Interaction of interleukin-6 and the BMP pathway in pulmonary smooth muscle. *Am J Physiol Lung Cell Mol Physiol* 2007; **292**: L1473–9.

Artificial
Organs

Atrionatriuretic Peptide Improves Left Ventricular Function After Myocardial Global Ischemia–Reperfusion in Hypoxic Hearts

Yasuhiro Fujii, [1]Kozo Ishino, Tomoko Tomii, Hitoshi Kanamitsu, Yasufumi Fujita, Hideya Mitsui, and Shunji Sano

Department of Cardiovascular Surgery, Okayama University Hospital, Okayama, Japan

Abstract: Atrionatriuretic peptide (ANP) is reported to be useful for attenuating myocardial ischemia–reperfusion injury and improving left ventricular function after reperfusion. However, ANP may be either ineffectual or harmful in cases where the myocardium has been chronically hypoxic since birth. This can be a result of the concomitant high levels of cyclic guanosine monophosphate (cGMP) produced within the myocardium. This study aimed to verify the validity of using ANP to improve left ventricular function after myocardial ischemia–reperfusion injury. For this purpose, a cyanotic congenital disease model that was developed using isolated rat hearts was used. Hearts were obtained from Sprague-Dawley rats that were housed from birth until 6 weeks of age either in a hypoxic environment with 13–14% FiO_2 (hypoxic group) or in ambient air (normoxic group). These hearts were subjected to 30 min of normothermic global ischemia followed by 30 min of reperfusion using the Langendorff technique. Left ventricular functional recovery in hearts administered ANP (0.1 μM) into the reperfusion solution was compared with those hearts that were not administered ANP in both hypoxic (without ANP: $n = 6$, with ANP: $n = 6$, with ANP and HS-142-1[an antagonist of ANP]: $n = 6$) and normoxic hearts (without ANP: $n = 6$, with ANP: $n = 6$). In the hypoxic hearts, ANP administration improved the percent recovery of the left ventricular developed pressure (76.3 ± 9.2% without ANP vs. 86.9 ± 6.7% with ANP), maximum first derivative of the left ventricular pressure (82.4 ± 1.1% without ANP vs. 95.8 ± 6.5% with ANP), and heart rate (85.6 ± 4.7% without ANP vs. 96.1 ± 5.2% with ANP) after reperfusion. The improvement and recovery of these cardiac functions were closely related to significantly increased levels of postischemic cGMP release after ANP administration. The effect of ANP was blocked by HS-142-1. The improvements observed in the hypoxic group were similar to those found in the normoxic group. ANP administration during reperfusion improved left ventricular function after myocardial acute global ischemia–reperfusion equally in both the chronically hypoxic and age-matched normoxic groups. **Key Words:** Atrial natriuretic factor—Hypoxia—Myocardium—Reperfusion.

Hospital mortality rates for surgeries involving the repair of cyanotic congenital heart defects have decreased dramatically. However, acute cardiac failure during the postoperative period remains one of the leading causes of death among these patients (1). Ischemia–reperfusion injury is one of the causative factors of postoperative acute cardiac failure and involves damage to cardiomyocytes, vascular smooth muscle cells, and endothelial cells (2). Therefore, identifying drugs that attenuate acute myocardial ischemia reperfusion is important in improving the clinical outcomes of cardiac surgery.

Certain drugs are listed as clinical candidates for the prevention of myocardial ischemia–reperfusion injury during cardiac surgery. Nitric oxide (NO) donors have been found to improve left ventricular function after normothermic global ischemia in normal rabbit hearts. We previously reported that 0.1 μM atrionatriuretic peptide (ANP) administered

doi:10.1111/j.1525-1594.2011.01358.x

Received February 2011; revised July 2011.

Address correspondence and reprint requests to Dr. Yasuhiro Fujii, Department of Cardiovascular Surgery, Okayama University Hospital, 2-5-1 Shikatacho, Kita-ku, Okayama city, Okayama 700-8558, Japan. E-mail: yasuhiro-f@live.jp

[1]Current address: Department of Cardiovascular Surgery, Showa University Northern Yokohama Hospital, 35-1, Chigasaki-chuo, Tsuzuki-ku, Yokohama city, Kanagawa, 224-8503, Japan.

during reperfusion following 30 min of normothermic global ischemia in an isolated normal rat heart model improves left ventricular function by increasing the rate of release of cyclic guanosine monophosphate (cGMP) (3).

However, there is a significant risk in concluding that the cardioprotective effects of these drugs are also useful to treat patients with chronic hypoxia because the myocardial response to these drugs in a chronically hypoxic heart may be different from those in a normoxic heart. In support of this, Baker et al. (4) reported that a NO donor does not improve left ventricular function after myocardial ischemia–reperfusion in rabbit hearts subjected to chronic hypoxia from birth; this indicates that NO donors do not exert a protective effect on chronically hypoxic hearts. Although the cause of the diminished cardioprotective effect is unknown, it may result from an overlapping mechanism of both the cardioprotective effect of a NO donor and chronic hypoxia. Chronic hypoxia has a cardioprotective effect against subsequent global ischemia (5,6); this effect is mediated by the activation of NO production and subsequent myocardial cGMP synthesis (4,6,7). Replicating the same cardioprotective effect may be of no benefit and may even be harmful. In contrast, the cardioprotective effect of ANP has a different mechanism from that of NO donors (8). However, it remains unclear whether ANP can additively improve left ventricular function after myocardial ischemia–reperfusion injury. Therefore, this study aimed to elucidate whether ANP improves left ventricular function after global myocardial ischemia–reperfusion in congenital hypoxic hearts.

MATERIALS AND METHODS

Congenital hypoxic rat heart model (hypoxia from birth)

Male Sprague-Dawley rats were used in this study. They were treated in compliance with the "Principles of Laboratory Animal Care," which was established by the National Society for Medical Research, and the "Guide for the Care and Use of Laboratory Animals," which was published by the US National Institutes of Health (NIH publication no. 85–23, revised 1996). This study was approved by the institutional ethics review board of Okayama University Hospital. To determine the effects of ANP on rat myocardium subjected to chronic hypoxia since birth, an original congenital cyanotic heart model was developed in rats. The rats of the hypoxic group were housed in a normobaric, hypoxic chamber from the time of birth until 6 weeks of age as described previously (9). The oxygen and carbon dioxide concentrations in the chamber were maintained at 13–14% and <0.4%, respectively, and continuously monitored using both a gas analyzer (ML206; ADInstruments, Sydney, Australia) and a commercially available software (PowerLab; ADInstruments). The hypoxic chamber humidity was maintained at <75%, and the temperature was maintained between 23 and 27°C with continuous hygrothermometer monitoring (TRH-7X; Shinyei, Kobe, Japan). To characterize the relationship between chronic hypoxia and ANP, a control group consisting of normoxic rats was housed in ambient air in the same environment for the same period; the effects of ANP administration were measured in these two groups. Both groups were kept in the same room under the same light–dark cycle. Rat chow and tap water were provided ad libitum.

Isolated perfused rat heart

The apparatus used for the perfusion of isolated rat hearts previously described by Hearse et al. (10) was modified and used for the experiments. This apparatus was designed to work in two interchangeable perfusion conditions: the unloaded and loaded modes. In the unloaded mode, the hearts were perfused through the aorta at a pressure of 80 cm H_2O and continued to beat independently. In the loaded mode, the hearts were perfused in the same fashion, but beat with external force; these hearts were not paced. The coronary effluent was discarded. The perfusate was a modified Krebs-Henseleit bicarbonate buffer (KHB: pH 7.4) containing 118.0 mM NaCl, 25.0 mM $NaHCO_3$, 2.5 mM $CaCl_2$, 1.2 mM $MgSO_4$, 4.7 mM KCl, 1.2 mM KH_2PO_4, and 11.0 mM glucose. The buffer was bubbled with 95% oxygen and 5% carbon dioxide gas at 38.0°C, to maintain the aortic partial pressure of oxygen >400 mm Hg: the buffer was filtered through a cellulose acetate membrane (pore size: 0.45 μm) to remove particulate contaminants (9).

The rats were anesthetized with an intraperitoneal injection of 50 mg/kg pentobarbital, and 100 IU/100 g body weight (BW) heparin was injected into the exposed right femoral vein. A blood sample was collected from the exposed left femoral vein to determine the hematocrit value (Htc) by using a blood gas analyzer (ABL 555: Radiometer, Copenhagen, Denmark). The heart was promptly harvested and then immersed in cold (4°C) heparinized KHB. The aorta was connected to the perfusion apparatus within 1 min of excision, and Langendorff perfusion was established. The pulmonary artery was incised to facilitate coronary drainage. The heart was then perfused in a retrograde manner under the perfusion

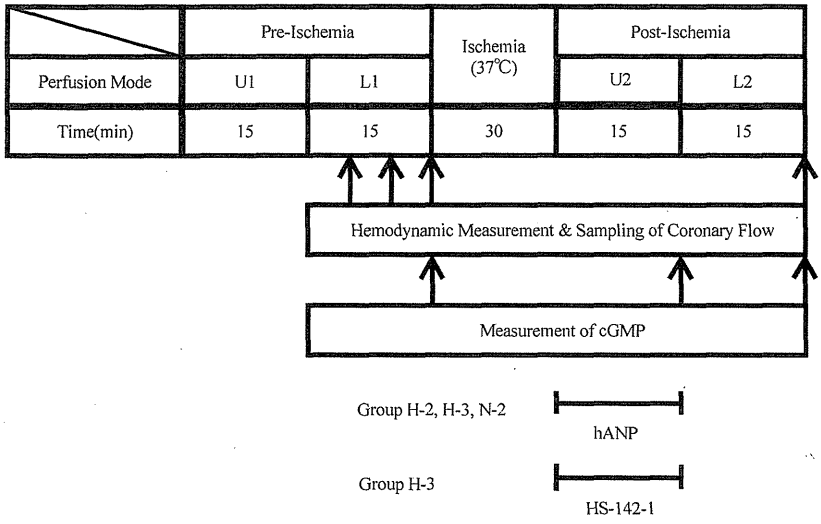

FIG. 1. Experimental protocol. cGMP, cyclic guanosine monophosphate; U, unloaded mode; L, loaded mode.

conditions of the unloaded mode at 38.0°C for 15 min. Changes in the heart rate (HR), left ventricular developed pressure (LVDP), and maximum first derivative of the left ventricular pressure (dP/dt max) were monitored in the loaded mode with PowerLab using an intraventricular balloon inserted through the mitral annulus and inflated with distilled water. During the pressure measurement, the left ventricular end-diastolic pressure was maintained at 4 mm Hg with the intraventricular balloon. The coronary flow (CF) was measured by direct collection of coronary effluent dripping from the heart for 1 min.

Study protocol

The experimental protocol is illustrated in Fig. 1. After an initial 15 min of washout (unloaded mode 1: U1), the hearts were perfused in the loaded mode for 15 min (loaded mode 1: L1). During this phase, HR, LVDP, dP/dt max, and CF were measured every 5 min, and the averages were recorded and assigned as the pre-ischemic indices. After 15 min of the loaded mode perfusion, the hearts were subjected to 30 min of global normothermic ischemia by clamping the aortic inflow line. Thirty minutes of global ischemia was selected because ischemia for periods exceeding 25 min induces sufficient myocardial damage (11). The sealed heart chamber temperature was monitored continuously during ischemia and maintained between 36.5 and 37.0°C. Hearts were reperfused for 15 min in the unloaded mode (unloaded mode 2: U2), followed by perfusion in the loaded mode for the next 15 min (loaded mode 2: L2). Postischemic cardiac function was evaluated at the end of this phase. The postischemic HR, LVDP, dP/dt max, and CF were calculated as percentages of their respective pre-ischemic values.

Thirty hearts were divided into five groups ($n = 6$ per group). In group H-1, the hearts of hypoxic rats were perfused without ANP. In group H-2, the hearts of hypoxic rats were perfused with 0.1 μM ANP (α-human atrionatriuretic peptide; Sankyo-Daiichi, Tokyo, Japan) during the U2 phase. In group H-3, the hearts of hypoxic rats were perfused with 0.1 μM ANP and 6 mg/L HS-142-1 (Kyowa Hakko Kogyo, Tokyo, Japan), a specific antagonist of the guanylyl cyclase ANP receptor during the U2 phase. In group N-1, the hearts of normoxic rats were perfused without ANP. In group N-2, the hearts of normoxic rats were perfused with 0.1 μM ANP during the U2 phase. In all groups, the release of cGMP into the CF was measured at the end of the L1, U2, and L2 phases.

The hearts were removed from the apparatus at the end of each experiment. The right ventricle (RV) and left ventricle (LV) were weighed separately. The interventricular septum was included in the LV. The ratio of wet RV/wet LV (RV/LV), wet RV/BW, and wet LV/BW were calculated. The hearts were heated to 70°C for 14 days and reweighed to determine the dry weight of the ventricular myocardium. The concentration of cGMP was determined by radioimmunoassay as described previously (12) and is expressed in picomoles per gram dry weight per min.

Exclusion criteria

Hearts presenting with HRs less than 250 beats/min after the first hemodynamic evaluation were excluded from the study because they were deemed

TABLE 1. *Characteristics of rats (final conditions and pre-ischemic values)*

Variable	Hypoxic groups			Normoxic groups	
	H-1 ($n = 6$)	H-2 ($n = 6$)	H-3 ($n = 6$)	N-1 ($n = 6$)	N-2 ($n = 6$)
BW (g)	154 ± 8*	167 ± 16**	164 ± 7***	207 ± 20	207 ± 12
Htc (%)	48 ± 3*	50 ± 7**	50 ± 2***	39 ± 3	39 ± 3
RV/LV	0.57 ± 0.11*	0.46 ± 0.04**	0.60 ± 0.08***	0.23 ± 0.01	0.24 ± 0.02
RV/BW (g/kg)	1.27 ± 0.33*	1.11 ± 0.28**	1.82 ± 0.29***	0.51 ± 0.05	0.50 ± 0.05
LV/BW (g/kg)	2.22 ± 0.23	2.38 ± 0.38	3.06 ± 0.11***	2.22 ± 0.31	2.08 ± 0.14
LVDP (mm Hg)	126 ± 7	121 ± 8	117 ± 5	122 ± 7	115 ± 9
dP/dt max (mm Hg/s)	3604 ± 187	3694 ± 570	3520 ± 286	4038 ± 341	3611 ± 223
HR (beat/min)	316 ± 13	291 ± 14	299 ± 24	312 ± 30	312 ± 22
CF (mL/min)	11.1 ± 3.3	9.6 ± 1.7	12.4 ± 1.6	7.6 ± 1.2	9.3 ± 2.3
cGMP (pmol/dry weight/min)	34.5 ± 13.0	38.7 ± 14.5	37.1 ± 12.6	15.3 ± 7.8	21.1 ± 20.4

Values are represented as mean ± standard deviation.
* $P < 0.05$, group H-1 vs. group N-1 and group H-1 vs. group N-2.
** $P < 0.05$, group H-2 vs. group N-1 and group H-2 vs. group N-2.
*** $P < 0.05$, group H-3 vs. group N-1 and group H-3 vs. group N-2.
BW, final body weight; CF, coronary flow; cGMP, cyclic guanosine monophosphate; dP/dt max, maximum first derivative of left ventricular pressure; HR, heart rate; Htc, hematocrit value; LV, left ventricular wet weight; LVDP, left ventricular developed pressure; RV, right ventricular wet weight.

to have sustained severe myocardial damage during the preparation.

Statistical analysis

All data are expressed as mean ± standard deviation. Statistical analysis was performed using commercially available software (SPSS Ver.19 for Windows; SPSS Japan, Tokyo, Japan). One-way analysis of variance (ANOVA) followed by Fisher's protected least significant difference test was used to compare data among the five groups. To determine the effect of ANP among the three hypoxic groups, one-way ANOVA followed by Scheffe's test was used. The interaction between ANP and chronic hypoxia with respect to myocardial ischemia–reperfusion injury was evaluated with a two-way ANOVA followed by Scheffe's test using the results of groups H-1, H-2, N-1, and N-2. A paired *t*-test was used to compare cGMP production in the CF of each group. A P value of <0.05 was regarded as statistically significant.

RESULTS

Pre-ischemic data

Table 1 shows the characteristics of the rats used in this study. The final BWs of the rats of the hypoxic groups were significantly lower than those of the normoxic groups. The pre-experimental Htc was significantly higher in the hypoxic groups than in the normoxic groups. The ratio of wet RV/wet LV was significantly higher in the hypoxic groups than in the normoxic groups. The wet RV/BW ratio was significantly higher in the hypoxic groups than in the normoxic groups. These results indicate that in the hypoxic groups, RV hypertrophy tends to be significantly more prevalent than LV hypertrophy. There were no statistically significant differences in HR, dP/dt max, and LVDP among the hypoxic groups. CF tended to increase in the hypoxic groups compared to the normoxic groups. The rate of cGMP drainage in CF tended to be greater in the hypoxic groups than in the normoxic groups. The average pre-ischemic cGMP drainage in CF was significantly larger in the hypoxic groups than in the normoxic groups ($P < 0.01$, 36.7 ± 12.7 vs. 20.3 ± 14.1 pmol/dry weight/min, respectively).

Postischemic cardiac functional recovery and changes in cGMP release rate

The postischemic recovery of LVDP, dP/dt max, HR, and CF are expressed as percentages of the pre-ischemic value and are listed in Table 2. The extent of the postischemic recovery of LVDP, dP/dt max, and HR was significantly better in group H-2 than in groups H-1 and H-3. There was no significant difference in the extent of cardiac function recovery between group H-1 and H-3. In the normoxic groups, the extent of postischemic recovery of LVDP, dP/dt max, and HR was greater in group N-2 than in group N-1. In the groups reperfused without ANP (group H-1 and N-1), the extent of postischemic recovery of LVDP, dP/dt max, and CF was significantly better in group H-1 than in group N-1.

Changes in the release of cGMP are shown in Fig. 2. The rate of cGMP release tended to be higher in the hypoxic rats than in the normoxic ones. In both the hypoxic and normoxic groups, the cGMP release occurring at the end of the U2 phase increased sig-

TABLE 2. *Postischemic recovery of left ventricular developed pressure, first derivative of left ventricular pressure, heart rate, and coronary flow*

	Hypoxic groups			Normoxic groups	
Variables	H-1 ($n = 6$)	H-2 ($n = 6$)	H-3 ($n = 6$)	N-1 ($n = 6$)	N-2 ($n = 6$)
LVDP (%)	76.3 ± 9.2†	86.9 ± 6.7*	76.8 ± 4.2**	66.0 ± 11.9	77.1 ± 7.3***
dP/dt max (%)	82.4 ± 1.1†	95.8 ± 6.5*	82.8 ± 13.4**	64.0 ± 12.5	83.1 ± 8.3***
HR (%)	85.6 ± 4.7	96.1 ± 5.2*	92.7 ± 11.1**	86.3 ± 8.4	96.5 ± 5.0***
CF (%)	96.6 ± 25.7†	92.4 ± 20.9	81.5 ± 3.8	79.5 ± 8.3	89.1 ± 30.3

Values are represented as mean ± standard deviation.
* $P < 0.05$, group H-1 vs. group H-2.
** $P < 0.05$, group H-2 vs. group H-3.
*** $P < 0.05$, group N-1 vs. group N-2.
† $P < 0.05$, group H-1 vs. group N-1.
CF, coronary flow; cGMP, cyclic guanosine monophosphate; dP/dt max, maximum first derivative of left ventricular pressure; HR, heart rate; LVDP, left ventricular developed pressure.

nificantly with ANP administration in groups H-2 and N-2. The release of cGMP in both groups decreased to pre-ischemic levels after the end of the L2 phase. There was no difference in the rate of cGMP release between groups H-1 and H-3 at any time point.

Postischemic cardiac functional recovery was closely correlated with a significantly increased rate of cGMP release as a result of ANP administration; this cardioprotective effect was blocked by a specific antagonist of the guanylyl cyclase ANP receptor.

Interaction between the cardioprotective effects of ANP and chronic hypoxia

The interactions between the effects of ANP and chronic hypoxia on cardiac function recovery are shown in Fig. 3. ANP administration improved the recovery of the LVDP (10.6% improvement in hypoxic hearts vs. 11.1% in normoxic hearts), dP/dt max (13.4% vs. 19.1%), and HR (10.5% vs. 10.2%) after reperfusion of both hypoxic and normoxic hearts to the same degree. No interaction was identified between ANP and chronic hypoxia with respect to the recovery of LVDP ($P = 0.9270$), dP/dt max ($P = 0.4045$), HR ($P = 0.9583$), and CF ($P = 0.5030$) using the two-way ANOVA followed by Scheffe's test.

DISCUSSION

Effect of ANP on congenitally hypoxic heart

The present study provides the first direct evidence that ANP improves left ventricular function after myocardial acute global ischemia–reperfusion equally, in both chronically hypoxic and normal

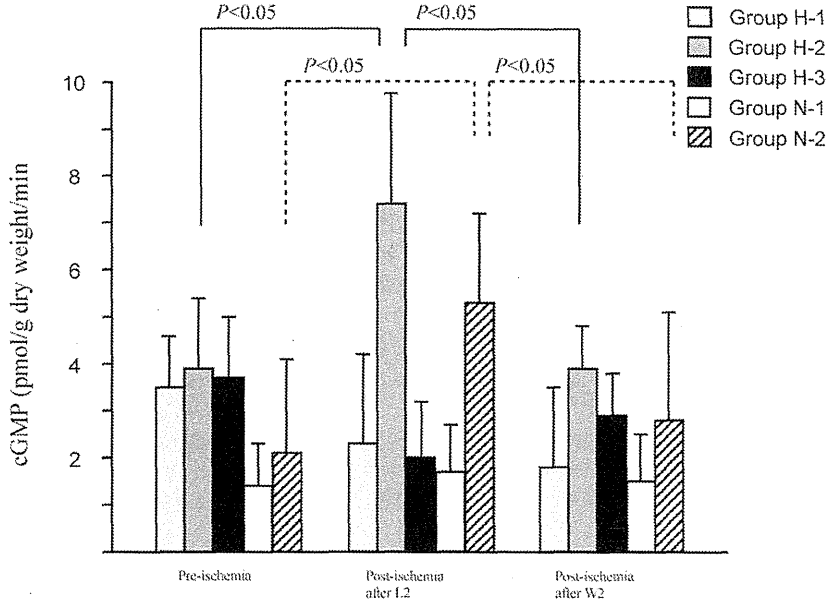

FIG. 2. Changes in cyclic guanosine monophosphate (cGMP) leakage. The rate of cGMP release tended to be higher in the hypoxic rats than in the normoxic rats. In groups H-2 and N-2 (both hypoxic and normoxic rats), cGMP was released at the end of the U2 phase and increased significantly with ANP administration. The release of cGMP in both groups decreased to the pre-ischemic levels after the end of the L2 phase. Bars represent standard deviation.

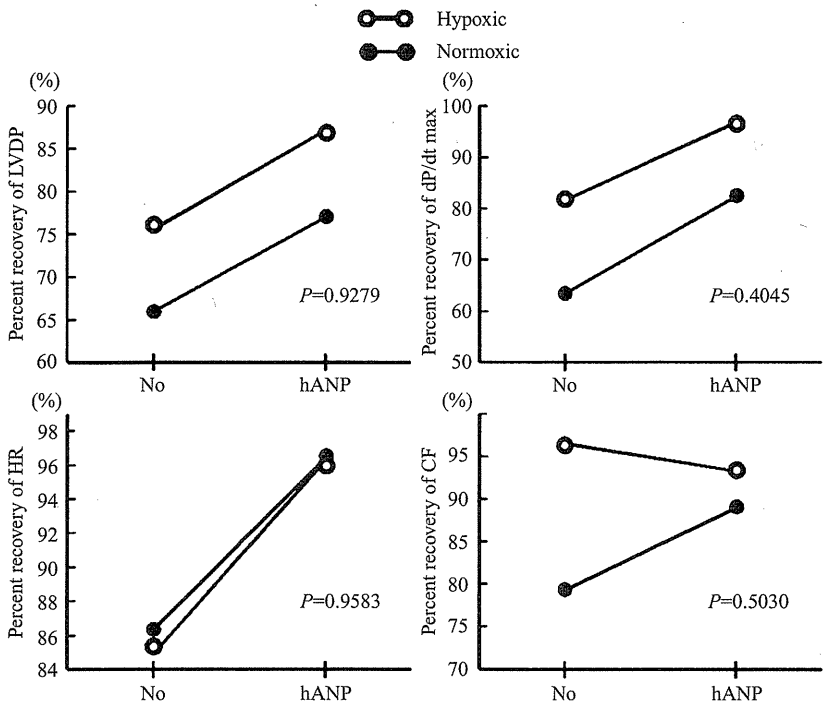

FIG. 3. Interactions between ANP and chronic hypoxia on left ventricular developed pressure, first derivative of left ventricular pressure, heart rate, and coronary flow. There was no interaction between ANP and chronic hypoxia from birth. LVDP, left ventricular developed pressure; dP/dt max, maximum first derivative of left ventricular pressure; HR, heart rate; CF, coronary flow; cGMP, cyclic guanosine monophosphate.

hearts. The increase in the release rate of cGMP following the initial 15 min of reperfusion and the lack of a cardioprotective effect in the presence of an ANP receptor blocker indicate that the protective effects of ANP against ischemia–reperfusion injury are partly mediated by the direct effect of cGMP on cardiomyocytes. ANP is known to activate a particulate guanylyl cyclase associated with the ANP receptor and increase the rate of intracellular cGMP synthesis (3). However, the relationship between the cGMP concentration in the reperfused myocardium and the extent of the protective effects against reperfusion injury is not known. It is suggested that overstimulation of cGMP synthesis could be detrimental to the reperfused myocardium and may result in increased apoptotic cell death (13). Padilla et al. (14) clearly demonstrated the negative effects of excessive cGMP in isolated rat hearts that received large doses of urodilatin (a member of the natriuretic peptide family) after 40 min of ischemia. Therefore, it is important to determine the doses of agents necessary to obtain the targeted increase in cGMP in the reperfused myocardium. In this study, 0.1 μM ANP was used because the previous study demonstrated that 0.1 μM ANP induces an increase in cGMP release without a significantly negative hemodynamic effect in normoxic rat hearts (3). The results of this study indicate that 0.1 μM ANP is an acceptable level even in chronically hypoxic hearts.

Interaction between ANP and chronic hypoxia

This study shows that ANP equally improves left ventricular function following an acute myocardial ischemia–reperfusion injury in chronically hypoxic and normal rat hearts. Our results are very different from those of Baker et al. who attempted to demonstrate that a NO donor exerts a cardioprotective effect against ischemia–reperfusion injury in chronically hypoxic hearts by using an isolated rabbit heart model. In that study, no improvement in left ventricular function after myocardial acute global ischemia–reperfusion was observed in rabbit hearts reperfused with the NO donor; this finding is in contrast with those in the rabbit hearts reperfused without NO donor (4).

The results of this study lead us to question why the cardioprotective effect of ANP was not diminished in hearts that were subjected to chronic hypoxia. Two potential reasons can be considered. First, the mechanisms activating cGMP synthesis may be different for ANP and chronic hypoxia. Hypoxia preconditioning is predominantly dependent upon increased NO synthesis; furthermore, increased NO levels directly activate soluble guanylyl cyclase. This mechanism for activating cGMP synthesis is the same as that used by the NO donor. On the other hand, ANP binds to the ANP receptor and indirectly activates the particulate guanylyl cyclase associated with the ANP receptor (8). Although both types of guanylyl cyclase activate

cGMP synthesis, the intramyocardial cGMP is known to be highly compartmentalized. Because these compartmentalized cGMPs often have different effects, chronic hypoxia (which involves soluble guanylyl cyclase-dependent cGMP synthesis) and ANP administration (which involves particulate guanylyl cyclase-dependent cGMP synthesis) may have different effects on the myocardium (8,15,16). Su et al. report that particulate guanylyl cyclase-dependent cGMP predominantly contributes to a decrease in intracellular Ca^{2+} levels, while soluble guanylyl cyclase-dependent cGMP predominantly contributes to a reduction in the sensitivity of myofilaments to Ca^{2+} (8).

ANP also appears to have an additional cardioprotective effect against myocardial ischemia–reperfusion injury. Another study provides evidence for the existence of an independently functioning and local renin–angiotensin system in the heart (17). In an isolated perfused rat heart, angiotensin II was found to exacerbate ischemia-induced ventricular fibrillation and to impair cardiodynamics; these effects were blocked by ANP (18). Morales et al. (19) report that directly blocking the local renin-angiotensin system with angiotensin II receptor antagonists relieves myocardial stunning after global ischemia. Therefore, the functional antagonism of angiotensin II may underlie the protective effect of ANP against ischemia–reperfusion injury. This cardioprotective effect of ANP, which is not related to cGMP, may therefore contribute to the further cardioprotective effects observed in the hypoxic hearts investigated in this study. Further study is needed to elucidate the full consequences of the interaction.

Study limitations

There are several limitations to the model system employed in this study. First, an isolated perfused preparation was used. Although the preparations were denervated, direct cardiac responses can be studied independent of the systemic effects of ANP. Second, a crystalloid solution was used in the perfusion circuit, which might have produced results different from those in a blood perfusion (20). The fact that various blood components play different roles during ischemia and reperfusion could have affected the results. Therefore, we used a simple crystalloid solution to simplify the study's model. Third, the animals were subjected to the protocol on the 1st day after birth. In contrast, children with cyanotic congenital heart disease are generally cyanotic since birth, having never been exposed to normoxia. Fourth, neonate animals were intermittently reoxygenated when they were exposed to air for feeding and maintenance. The effect of such brief normoxia has not yet been clarified. Finally, it should be noted that this study does not confirm that ANP is safe for use in clinical situations involving acute ischemia–reperfusion of chronic hypoxic hearts. The experimental conditions of this study have many differences from clinical situations. Further study is required to evaluate the validity of the findings for applications in patients with congenital hypoxia.

CONCLUSION

Atrionatriuretic peptide administration during the reperfusion of congenital hypoxic rat hearts following global ischemia improved the recovery of left ventricular function to the same degree as age-matched normal rat hearts. Although ANP and chronic hypoxia increased the rate of myocardial cGMP synthesis, there appears to be no interaction between ANP and chronic hypoxia with respect to their beneficial effects on left ventricular function following ischemia–reperfusion. These results indicate that ANP may have a cardioprotective pathway independent of its promotion of cGMP synthesis.

Acknowledgments: We thank Sankyo-Daiichi and Kyowa Hakko Kogyo for generously donating the α-human atrionatriuretic peptide and HS-142-1.

REFERENCES

1. Kirklin JW, Barratt-Boyes BG. Ventricular septal defect and pulmonary stenosis or atresia. In: Kirklin JW, Barratt-Boyes BG, eds. *Cardiac Surgery*, 3rd Edition. New York: Churchill Livingstone, 1993;861–1012.
2. Murphy GJ, Angelini GD. Side effects of cardiopulmonary bypass: what is the reality? *J Card Surg* 2004; 19:481–8.
3. Sangawa K, Nakanishi K, Ishino K, Inoue M, Kawada M, Sano S. Atrial natriuretic peptide protect against ischemia-reperfusion injury in the isolated rat heart. *Ann Thorac Surg* 2004;77:233–7.
4. Baker JE, Holman P, Kalyanaraman B, Griffith OW, Pritchard KA. Adaptation to chronic hypoxia confers tolerance to subsequent myocardial ischemia by increased nitric oxide production. *Ann N Y Acad Sci* 1999;874:236–53.
5. Baker EJ, Boerboom LE, Olinger GN, Baker JE. Tolerance of the developing heart to ischemia: impact of hypoxemia from birth. *Am J Physiol* 1995;268:H1165–73.
6. Fujii Y, Ishino K, Tomii T, Kanamitsu H, Mitsui H, Sano S. Tolerance of the developing cyanotic heart to ischemia-reperfusion injury in the rat. *Gen Thorac Cardiovasc Surg* 2010;58:174–81.
7. Baker JE, Contney SJ, Singh R, Kalyanaraman B, Gross GJ, Bosnjak ZJ. Nitric oxide activates the sarcolemmal K(ATP) channel in normoxic and chronically hypoxic hearts by a cyclic GMP-dependent mechanism. *J Mol Cell Cardiol* 2001;33:331–41.

8. Su J, Scholz PM, Weiss HR. Differential effects of cGMP produced by soluble and particulate guanylyl cyclase on mouse ventricular myocites. *Exp Biol Med* 2005;230:242–50.
9. Nakanishi K, Inoue M, Sugawara E, Sano S. Ischemia and reperfusion injury of cyanotic myocardium in chronic hypoxic rat model: changes in cyanotic myocardial antioxidant system. *J Thorac Cardiovasc Surg* 1997;114:1088–96.
10. Hearse DJ, Stewart DA, Braimbridge MV. Hypothermic arrest and potassium arrest. *Circ Res* 1975;36:481–9.
11. Wang QD, Swardh A, Sjoquist PO. Relationship between ischemic time and ischemia/reperfusion injury in isolated Langendorff-perfused mouse hearts. *Acta Physiol Scand* 2001;171:123–8.
12. Steiner AW, Parker CW, Kipnis DM. Radioimmunoassay for cyclic nucleotides 1. Preparation of antibodies and iodinated cyclic nucleotides. *J Biol Chem* 1972;247:1106–13.
13. Taimor G, Hofstaetter B, Piper HM. Apoptosis induction by nitric oxide in adult cardiomyocytes via cGMP-signaling and its impairment after simulated ischemia. *Cardiovasc Res* 2000;45:588–99.
14. Padilla F, Garcia-Dorado D, Agullo L, et al. Intravenous administration of the natriuretic peptide urodilatin at low doses during coronary reperfusion limits infarct size in anesthetized pigs. *Cardiovasc Res* 2001;51:592–600.
15. Castro LR, Verde I, Cooper DM, Fischmeister R. Cyclic guanosine monophosphate compartmentation in rat cardiac myocytes. *Circulation* 2006;113:2221–8.
16. Piggott LA, Hassell KA, Morris AP, Silberbach M, Rich TC. Natriuretic peptides and nitric oxide stimulate cGMP synthesis in different cellular compartment. *J Gen Physiol* 2006;128:3–14.
17. Lindpaintner K, Wilhelm MJ, Jin M, et al. Tissue renin-angiotensin systems: focus on the heart. *J Hypertens* 1987;5:S33–8.
18. Linz W, Scholkens BA, Albus U, Petry P, Breipohl G, Knolle J. Atrial natriuretic factor protects the isolated working ischemic rat heart against the action of angiotensin II. *J Hypertens* 1988;6:S339–41.
19. Morales C, Rodriguez M, Scapin O, Gelpi RJ. Comparison of the effects of ACE inhibition with those of angiotensin II receptor antagonism on systolic and diastolic myocardial stunning in isolated rabbit heart. *Mol Cell Biochem* 1998;186:117–21.
20. Walters HL III, Digerness SB, Naftel DC, Waggoner JR III, Blackstone EH, Kirklin JW. The response to ischemia in blood perfused versus crystalloid perfused isolated rat heart preparations. *J Mol Cell Cardiol* 1992;24:1063–7.

DOI: 10.1111/j.1540-8175.2011.01600.x

Echocardiography

Transcatheter Closure of a Large Atrial Septal Defect under Microprobe Transesophageal Echocardiographic Guidance

Manabu Taniguchi, M.D.,* Teiji Akagi, M.D.,* Yasufumi Kijima, M.D.,† Hiroshi Ito, M.D.,† and Shunji Sano, M.D.*

*Division of Cardiac Intensive Care Unit, Okayama University Hospital, Okayama, Japan; †Department of Cardiovascular Medicine, Okayama University Graduate School of Medicine, Dentistry and Pharmaceutical Sciences, Okayama, Japan

We present a case of an atrial septal defect (ASD) in a 59-year-old man with an indication for ASD closure who also had a history of chronic obstructive pulmonary disease. Because of his decreased respiratory function with multiple bullae in his lungs, the procedure was performed without general anesthesia under the guidance of fluoroscopy and two-dimensional (2D) transesophageal echocardiography (TEE) using a transesophageal echocardiographic microprobe (micro-TEE) (S8-3t; Philips Medical Systems, Andover, MA, USA). The micro-TEE probe was inserted into the esophagus smoothly and easily in the supine position without sedation. It revealed a deficient superior-anterior rim and adequate rims elsewhere, and the maximal diameter of ASD was measured to be 25 mm. Balloon sizing resulted in a stretched defect diameter of 29 mm using the stop-flow technique. A 30-mm AMPLATZER Septal Occluder (AGA Medical, Plymouth, MN, USA) was deployed. The micro-TEE demonstrated that both disks were on the appropriate sides of the interatrial septum and the device was not interfering with surround cardiac structures. Residual shunt flow was not detected with color Doppler. The device was released successfully without any complications. Recently introduced multiplane micro-TEE can provide adequate information about a large ASD with a less invasive procedure in adult patients. Micro-TEE has a potential to become a novel imaging option for interventions of the interatrial septum. (Echocardiography 2012;29:E94-E96)

Key words: transesophageal echocardiography, atrial septal defect, transcatheter closure device

A 59-year-old man with a history of chronic obstructive pulmonary disease who presented with progressive exertional dyspnea was found to have a secundum-type atrial septal defect (ASD) and a dilated right ventricle on transthoracic echocardiography (TTE). He was referred to our hospital for evaluation and transcatheter ASD closure.

Right heart catheterization demonstrated a pulmonary-to-systemic flow ratio of 1.8:1. His respiratory function was decreased due to multiple bullae in his lungs. And an intracardiac echocardiography was unavailable in our hospital. Therefore, transcatheter ASD closure was performed without general anesthesia under the guidance of fluoroscopy and two-dimensional (2D) transesophageal echocardiography (TEE) using a transesophageal echocardiographic microprobe (micro-TEE) (S8-3t; Philips Medical Systems, Andover, MA, USA) (Fig. 1). No sedatives were used, and local pharyngeal anesthesia was induced with oral liquid containing lignocaine. The micro-TEE probe was inserted into the

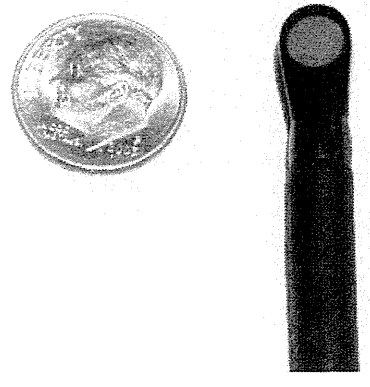

Figure 1. Miniaturized micro-TEE probe.

There are no disclosures about this report.

Address for correspondence and reprint requests: Manabu Taniguchi, M.D., PHD 2-5-1 Shikata-Cho, Okayama Kita-ku, Okayama 700-8558, Japan. Fax: 81-86-235-7353; E-mail: tmnb@md.okayama-u.ac.jp

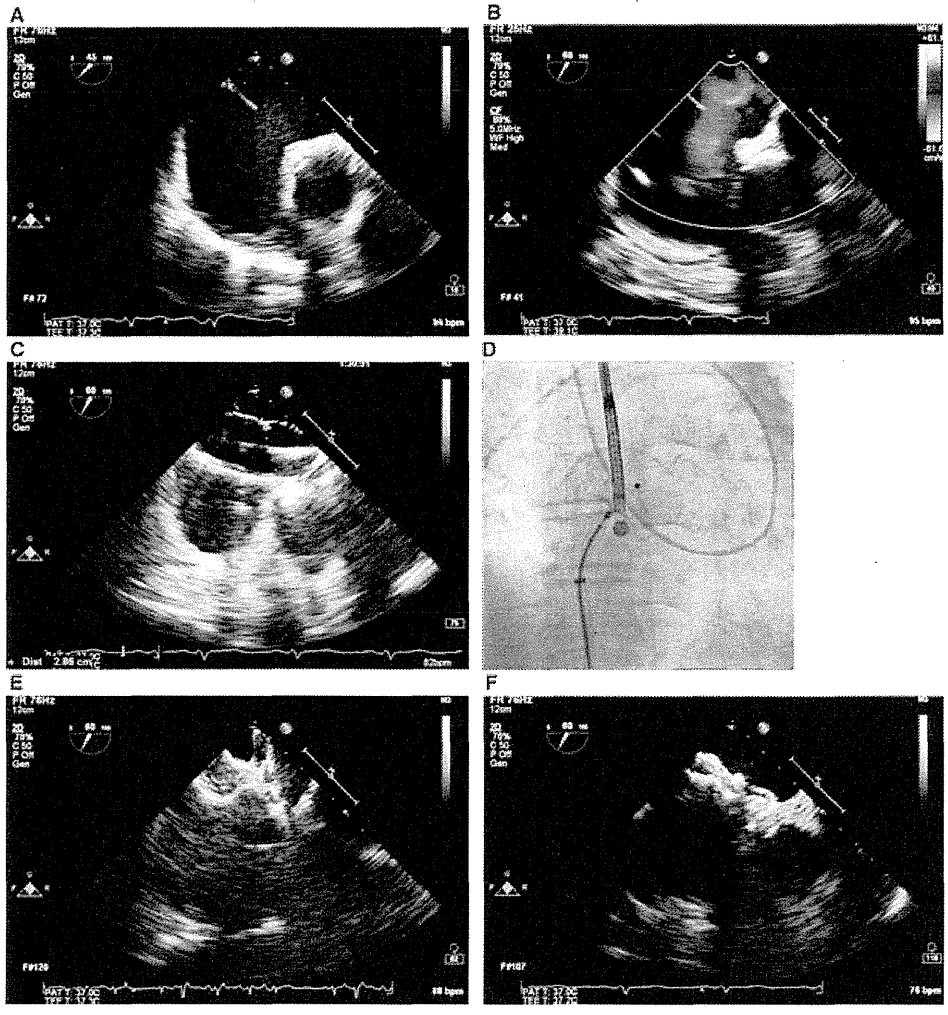

Figure 2. Transcatheter atrial septal defect closure under micro-TEE and fluoroscopic guidance. **A.** Micro-TEE demonstrates a large atrial septal defect (ASD) and a deficient superior-anterior rim. **B.** With color Doppler image, left-to-right shunt flow is recognized. **C.** Balloon sizing using the stop-flow technique **D.** Fluoroscopic view and **E.** micro-TEE view deploying a 30-mm AMPLATZER Septal Occluder **F.** Device is deployed successfully.

esophagus smoothly and easily in the supine position. It revealed a deficient superior-anterior rim and adequate rims elsewhere (Fig. 2A and B, movie clip S1), and the maximal diameter of ASD was measured to be 25 mm. Balloon sizing with a 34-mm AGA balloon (AGA Medical, Plymouth, MN, USA) resulted in a stretched defect diameter of 29 mm using the stop-flow technique (Fig. 2C). A 12-French AGA sheath was used to deliver the device. A 30-mm AMPLATZER Septal Occluder (AGA Medical, Plymouth, MN, USa) was deployed (Fig. 2D and E, movie clip S2). The micro-TEE clearly demonstrated that both disks were on the appropriate sides of the interatrial septum and the device was not interfering with surround cardiac structures. Residual shunt flow was not detected with color Doppler. The device was released successfully without any complications (Fig. 2F).

The extremely miniaturized multiplane micro-TEE has 18.5 mm of tip length, 7.5 mm of tip width, and 5.5 mm of tip height. The shaft size is 5.2 mm which is about a half size of the standard TEE probe for adults. The transducer consisted of 32 elements and has frequency from 3.2 MHz to 7.4 MHz. 2D, as well as M-mode, color Doppler, pulse-wave wave Doppler, and continuous-wave Doppler are available.

Echocardiography plays a pivotal role in guiding interventions of structural heart diseases. There are several imaging tools of echocardiographic guidance for structural heart interventions including 2D TTE, 2D TEE,[1] intracardiac echocardiography,[2,3] and recently introduced

real-time three-dimensional (3D) TEE.[4,5] From the standpoint of echocardiographic options for transcatheter closure of an interatrial septum in the catheterization laboratory, the small size of the micro-TEE probe may be better tolerated without general anesthesia for a prolonged procedure such as ASD closure, as compared to a standard TEE probe. In addition, micro-TEE has some advantages compared to intracardiac echocardiography in terms of capability of multiplane, reusability, avoiding vascular complications and cost effectiveness. However, image quality of the current micro-TEE probe is inferior to that of a conventional adult TEE probe, and inability of 3D imaging by a micro-TEE probe can also be a limitation.

Micro-TEE could provide adequate information with a less invasive procedure even in patients with a large ASD. Micro-TEE has the potential to become a novel imaging option for interventions of the interatrial septum.

References

1. Mazic U, Gavora P, Masura J: The role of transesophageal echocardiography in transcatheter closure of secundum atrial septal defects by the Amplatzer septal occluder. *Am Heart J* 2001;142:482–488.
2. Kim SS, Hijazi ZM, Lang RM, et al: The use of intracardiac echocardiography and other intracardiac imaging tools to guide noncoronary cardiac interventions. *J Am Coll Cardiol* 2009;53:2117–2128.
3. Ali S, George LK, Das P, et al: Intracardiac echocardiography: Clinical utility and application. *Echocardiography* 2011;28:582–590.
4. Taniguchi M, Akagi T, Watanabe N, et al: Application of real-time three-dimensional transesophageal echocardiography using a matrix array probe for transcatheter closure of atrial septal defect. *J Am Soc Echocardiogr* 2009;22:1114–1120.
5. Eng MH, Salcedo EE, Quaife RA, et al: Implementation of real time three-dimensional transesophageal echocardiography in percutaneous mitral balloon valvuloplasty and structural heart disease interventions. *Echocardiography* 2009;26:958–966.

Supporting Information

Additional Supporting Information may be found in the online version of this article:

Movie clip S1: Short-axis view with micro-TEE shows a large atrial septal defect (ASD) and a deficient superior-anterior rim.

Movie clip S2: The micro-TEE shows that both disks are on the appropriate sides of the interatrial septum.

Please note: Wiley-Blackwell are not responsible for the content or functionality of any supporting materials supplied by the authors. Any queries (other than missing material) should be directed to the corresponding author for the article.

DOI: 10.1111/joic.12002

STRUCTURAL HEART DISEASE

Long-Term Effects of Transcatheter Closure of Atrial Septal Defect on Cardiac Remodeling and Exercise Capacity in Patients Older than 40 Years with a Reduction in Cardiopulmonary Function

YOICHI TAKAYA, M.D.,[1] MANABU TANIGUCHI, M.D.,[2,3] TEIJI AKAGI, M.D.,[2] SAORI NOBUSADA, M.T.,[4] KENGO KUSANO, M.D.,[1] HIROSHI ITO, M.D.,[1] and SHUNJI SANO, M.D.,[2,5]

From the [1]Department of Cardiovascular Medicine, Okayama University Graduate School of Medicine, Dentistry and Pharmaceutical Sciences, Okayama, Japan; [2]Division of Cardiac Intensive Care Unit, Okayama University Hospital, Okayama, Japan; [3]Division of Cardiovascular Medicine, Fukuyama Cardiovascular Hospital, Fukuyama, Japan; [4]Division of Central Clinical Laboratory, Okayama University Hospital, Okayama, Japan; and [5]Department of Cardiovascular Surgery, Okayama University Graduate School of Medicine, Dentistry and Pharmaceutical Sciences, Okayama, Japan

Background: *Although it has been demonstrated that cardiac remodeling and exercise capacity improve after transcatheter closure of atrial septal defect (ASD), little is known about long-term benefits in middle-aged and elderly patients with a reduction in cardiopulmonary function.*
Objectives: *To evaluate long-term extent and time course of improvements in cardiac remodeling and exercise capacity in those patients.*
Methods: *Twenty ASD patients ≥ 40 years of age with a reduction in cardiopulmonary function (predicted peak oxygen uptake [VO_2] < 65%) were enrolled. Transthoracic echocardiography and cardiopulmonary exercise testing were performed at baseline and at 1 month, 3 months, 6 months, and >12 months after the procedure.*
Results: *At 1 month after the procedure, significant decreases in right ventricular (RV) end-diastolic diameter (38.2 ± 4.4 to 31.9 ± 4.4 mm; $P < 0.001$) and RV/left ventricular end-diastolic diameter ratio (0.95 ± 0.17 to 0.71 ± 0.13; $P < 0.001$) occurred, and they were maintained during the follow-up period. Normal RV size was achieved in 11 of 18 patients with RV enlargement. Predicted peak VO_2 did not change at 1 month and 3 months, but it improved significantly after 6 months (53.6 ± 6.5 to 62.1 ± 12.6%; $P < 0.01$). Sixteen of the 20 patients showed improved predicted peak VO_2.*
Conclusions: *Cardiac remodeling and exercise capacity could be improved over the long-term period after transcatheter closure of ASD in middle-aged and elderly patients with a reduction in cardiopulmonary function. There were differences in the time course of improvement between cardiac remodeling and exercise capacity in those patients.* (J Interven Cardiol 2013;26:195–199)

Introduction

Atrial septal defect (ASD) of secundum type is one of the most common forms of congenital heart disease in adults. Many patients with ASD are usually asymptomatic in early life, but clinical symptoms such as fatigue and dyspnea develop frequently in the course of time.[1,2] The development of clinical symptoms, echocardiographic signs of shunt volume or shunt-related pulmonary hypertension are widely accepted indications for closure of ASD. It is well known that surgical closure of ASD leads to long-term functional benefits in middle-aged and elderly symptomatic patients.[3–6] In recent years, transcatheter closure of ASD has been established as a secure and effective treatment, and it has become an important alternative to surgical repair for ASD.[7,8] A few studies

Conflict of interest: None

Address for reprints: Manabu Taniguchi, M.D., 2–39 Midorimachi, Fukuyama-shi, Hiroshima 720-0804, Japan. Fax: +81-84-925-9650; e-mail: tmnb@hotmail.com

have shown short-term benefits of transcatheter closure of ASD on cardiac remodeling and exercise capacity in middle-aged and elderly patients.[9,10] However, little is known about long-term results. Furthermore, the extent and time course of functional improvements after the procedure in middle-aged and elderly patients with a marked reduction in cardiopulmonary function remains unclear. Therefore, the aim of this study was to investigate the long-term extent and time course of improvements in cardiac remodeling and exercise capacity after transcatheter closure of ASD in those patients.

Methods

Study Population. From June 2006 to April 2009, 20 consecutive ASD patients $\geq$ 40 years of age with a moderate or severe reduction in cardiopulmonary function who underwent transcatheter closure of secundum ASD were enrolled. We defined moderate reduction in cardiopulmonary function as 50% $\leq$ predicted peak oxygen uptake (VO_2) < 65%, and we defined severe reduction as predicted peak VO_2 < 50%. The indications for ASD closure in all patients were significant left-to-right shunt detected by echocardiography, presence of right ventricular (RV) volume overload, shunt-related symptoms, or pulmonary hypertension. Exclusion criteria included pulmonary vascular resistance > 8 wood units on 100% O_2 and transesophageal maximal ASD diameter > 40 mm. The Okayama University Ethics Committee approved this study, which was performed in accordance with the Helsinki declaration, and all patients provided written informed consent before participation in this study.

Transcatheter Closure of ASD. Transesophageal echocardiography was performed in all patients before the procedure, and left atrial thrombi were not detected in any of the patients. Coronary angiography was performed in all patients, and there was no significant coronary stenosis. Transcatheter closure of ASD using an AMPLATZER septal occluder device (AGA Medical Corporation; Plymouth, MN, USA) was performed under general anesthesia with the assistance of transesophageal echocardiography. Hemodynamic evaluation was performed just before ASD closure. With oxygen uptake measured at rest, the pulmonary to systemic flow ratio was calculated by oxymetry using the Fick principle. If the pulmonary wedge pressure increased > 5 mmHg from baseline, the procedure was abandoned.

Echocardiography. Transthoracic echocardiography was performed at baseline and at 1 month, 3 months, 6 months, and >12 months after the procedure using a 3.5 MHz transducer (Aplio, Toshiba, Otawara, Japan). Left ventricular (LV) end-diastolic diameter, LV end-systolic diameter, and RV end-diastolic diameter were measured by M-mode parasternal echocardiography, and RV/LV end-diastolic diameter ratio was calculated. LV ejection fraction was derived using Teichholz's formula. These measurements were done at least three times and averaged to obtain mean values by 2 independent experienced investigators who were blinded to the data of treatment.

Cardiopulmonary Exercise Testing. Cardiopulmonary exercise testing was performed at baseline and at 1 month, 3 months, 6 months, and >12 months after the procedure. All patients underwent symptom-limited exercise tests on an upright bicycle ergometer using a ramp protocol (15 W/min) with simultaneous respirator gas analysis. Patients were encouraged to exercise to exhaustion or to a respiratory exchange ratio $\geq$ 1.09. Blood pressure and heart rate were measured every minute. A 12-lead electrocardiogram was continuously monitored during exercise testing. Breathed gas was continuously collected to analyze VO_2, carbon dioxide production, and minute ventilation with a gas analyzer. Peak VO_2 was defined as the highest VO_2 value achieved at peak exercise after reaching the respiratory compensation point, and predicted peak VO_2 was expressed according to age, sex, weight, and height. VO_2 to work rate ratio ($\Delta VO_2/\Delta WR$) was determined. A spirometric measurement was performed to assess vital capacity and forced expiratory volume in 1 second. These analyses were done by 2 independent experienced investigators who were blinded to the data of treatment.

Statistical Analysis. Variables are expressed as means $\pm$ standard deviation or percentage. Statistical analysis was performed by Wilcoxon's matched-pairs test. A P value < 0.05 was considered to be statistically significant.

Results

Study Population. Patient clinical characteristics are summarized in Table 1. Mean age at transcatheter closure of ASD was 54.5 $\pm$ 10.9 years (range, 40–78 years). Fourteen patients (70%) were female. ASD diameter measured by transesophageal echocardiography was 17.8 $\pm$ 4.3 mm. Pulmonary to